Transactions of the Nigerian Association of Mathematical Physics
Volume 14, (January - March, 2021 Issue), pp37 –46

ESTIMATION OF FREQUENCY, LUMINOSITY, AND THE EXPECTED TIME OF MERGER OF GRAVITATIONAL WAVE GENERATED BY BINARY BLACK HOLES.

[1]Bringen B., [2]Girma D. P. and [3]Bakwa D. D.

[1] Department of Physics, Faculty of Science, Borno State University,
[2]GSS Bet-Pankshin, Plateau State
[3]Department of Physics, Faculty of Natural Sciences, University of Jos

Abstract

GWs are predicted by any theory which assumes that gravitational effect propagate at finite speed. Characteristics such as the GW polarization, phase, and amplitude change depending on the theory assumed. It is for this reason that GWs can be used to test general relativity and explore the physics of objects such as black holes. The estimated values of frequency, luminosity, and time of merger of binary black holes (selected binary systems: PSR 1913+16, XTE J1118+480, 1915+105, Nova Scopii, V4641 Sgr, and VFTS 352 and their companions) obtained from different galaxies with qualitative behavior of compact binary coalescences within the post-Newtonian framework, using the parameters considered includes the distance r (observer distance), R (orbital separation), masses M ($M_{\odot}$);the results obtained from the estimation of binary black hole parameters are presented in tables 1, 2, and 3. The results indicate a high sensitivity that could be suitable within the detector's frequency band, such as LISA. The values indicate that these BBH are suitable candidates for GW detectors. The estimated values of frequencies of 10^{-5} – 10^{-7}Hz shows an excellent sensitivity for LISA. The LIGO's system reached a peak gravitational-wave luminosity of 3.6 x 10^{56}erg/s equivalent to $200M_{\odot}C^2$. Meanwhile the estimated values obtained as shown in figure 2 is between 145.8 x 10^{50} - 0.717 x10^{50} erg/s which gives a significant gravitational- wave luminosity of the sources BBH. Meanwhile, the estimated time of merger for the source stars indicated in table 3 reveals to be between10^{12} - 10^{20}s. The LIGO observatories has a range of detectable signals of GW amplitude as h ~ 1.0 x10^{-21} and h ~ 3.3 x10^{-22} when GW150914 and GW151226 were detected. These observations were made at signal frequencies of f ~ 35 – 350 Hz and 35 – 450 Hz by the aLIGO.

Key Words: Frequency, luminosity, merger, Gravitational wave, Binary black holes

1. Introduction

Waves are a well-known phenomenon in Physics. Oscillating matter can cause waves that carry its energy away. In our daily life we can see the mechanical waves in water when one throws a stone in a pond or hear the sound waves caused by oscillating snares. Physically understanding these waves comes very natural to us. Energy stored in waves can be felt when you are blown away by a large sound system or when a tsunami wipes down a village.

Gravity is the weakest of the four fundamental forces, but it is responsible for shaping our Universe. Our current understanding is based on Einstein's theory of General Relativity (GR), which describes the interaction between masses, or more general energy, with space and time [1]. It agrees with Newtonian gravity where applicable, but also predicts phenomena that go well beyond the Newtonian picture. One such phenomenon is the occurrence of gravitational radiation, called gravitational waves (GWs). These waves are perturbations of spacetime itself, produced by accelerated masses, which distort the fabric of spacetime in their vicinity. These distortions propagate away from the source at the speed of light. Analogously to electromagnetic radiation, GWs carry physical information and can therefore be regarded as "fingerprints" of the generating source revealing its true nature, which opens a new window to the Universe [2].

Correspondence Author: Bringen B., Email: bbringen@yahoo.com, Tel: +2348029771793

Astrophysical sources of gravitational radiation include inspiraling double compact objects, binary stars, rotating neutron stars (NSs), neutron star instabilities, supernovae, supermassive black holes (SMBHs), and stochastic background. Some of the most promising candidates are the inspiral and coalescence of double compact objects (DCOs), such as NS-NS, BH-NS, and BH-BH binaries. Successful detection of these sources at reasonable event rates depends not only on the instrument sensitivity and the strength of the gravitational-wave signals but also on the coalescence rates and the physical properties of the sources out to the maximum distances of reach of a given instrument. [3].

Mergers of comparable-mass black-hole binaries are among the strongest sources of gravitational waves. This final death spiral of a black-hole binary encompasses three stages: inspiral, merger, and ringdown [4]. In the early stages of the inspiral, the orbits of most astrophysical black-hole binaries will circularize due to the emission of gravitational radiation [5]. During the inspiral, the orbital time scale is much shorter than the time scale on which the orbital parameters change; consequently, the black holes spiral together on quasicircular orbits. Since the black holes have wide separations, they can be treated as point particles.

The inspiral phase produces gravitational waves in the characteristic form of a chirp, which is a sinusoid with both frequency and amplitude increasing with time. As the black holes' spiral inward, they eventually reach the strong-field, dynamical regime of general relativity. In this merger stage, the orbital evolution is no longer quasi-adiabatic; rather, the black holes plunge together and coalesce into a single, highly distorted remnant black hole, surrounded by a common horizon. Finally, the highly distorted remnant black hole settles down into a quiescent rotating Kerr black hole by shedding its non-axisymmetric modes through gravitational wave emission. We call this process the "ringdown," [6].

GWs are predicted by any theory which assumes that gravitational effect propagate at finite speed. Characteristics such as the GW polarization, phase, and amplitude change depending on the theory assumed. It is for this reason that GWs can be used to test general relativity. In addition, they can be used to explore the physics of objects such as black holes, gamma-ray bursts, and supernovae above and beyond the information currently available from astronomy [7].

As GWs pass through space, space is contracted and expanded in directions orthogonal to the direction of propagation. According to GR, the GW can be decomposed into a linear combination of two transverse polarizations, known as plus and cross. Assuming the direction of propagation is along the z-axis, the plus polarization occurs in the x and y-directions and the cross along the two diagonals. The plus and cross components of GWs are exploited to detect them with interferometric detectors [7]

There are alternative theories, however, which predict the existence of up to 6 polarizations. For the purposes of this research, we will explore only the plus and cross polarizations. Again, assuming the propagation is along the z-axis, the scalar polarization stretches the x-y space the directions, as shown in figure 1.

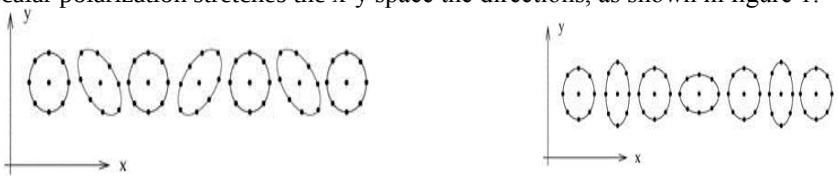

Fig. 1 The deformation of space in the x and y-directions by a GW with a plus polarization and a cross polarization

2.0 General Relativity in a Nutshell

In 1916, the year after the final formulation of the field equations of general relativity, Albert Einstein predicted the existence of gravitational waves. He found that the linearized weak-field equations had wave solutions: transverse waves of spatial strain that travel at the speed of light, generated by time variations of the mass quadrupole moment of the source. Einstein understood that gravitational-wave amplitudes would be remarkably small; moreover, until the Chapel Hill conference in 1957 there was significant debate about the physical reality of gravitational waves [8]. He came to appreciate these aspects of the theory over the next several years while working with mathematician Hermann Minkowski (1864–1909). Minkowski developed the idea of spacetime, in which events occur in a four-dimensional "space" that includes both (the three dimensions of) space and (one more dimension of) time. i.e. $x^{\mu} = (t, x, y, z)$

This is given by $\boldsymbol{\eta_{\mu\nu}} = \begin{pmatrix} -1 & 0 & 0 & 0 \\ 0 & 1 & 0 & 0 \\ 0 & 0 & 1 & 0 \\ 0 & 0 & 0 & 1 \end{pmatrix}$. (1)

In special relativity the interval, ds^2 between two events on the spacetime manifold is given by

$$\boldsymbol{ds^2 = \eta_{\mu\nu} dx^{\mu} dx^{\nu}} \quad (2)$$

And then in general relativity the interval between two events in spacetime is defined by a general metric, $\boldsymbol{g}$

$$\boldsymbol{ds^2 = g_{\mu\nu} dx^{\mu} dx^{\nu}} \quad (3)$$

In February 1916, Schwarzschild submitted the spherically symmetric solution.

$$\boldsymbol{ds^2 = -\left(1 - \frac{2M}{r}\right) dt^2 + \frac{1}{\left(1 - \frac{2M}{r}\right)} dr^2 + r^2 d\theta^2 + r^2 sin^2\theta d\varphi^2} \quad (4)$$

with matter-the "interior Schwarzschild solution"-now based on Einstein's final field equation. The field equation used by Schwarzschild requires det $g = -1$. To fulfill this condition, he uses modified polar coordinates that were later understood to describe a black hole [9].

In 1963 Kerr generalized the solution to rotating black holes as

$$\boldsymbol{ds^2 = -\left(1 - \frac{2M}{r}\right)(dv - asin^2\theta\varphi)^2 + 2(dv - asin^2\theta\varphi)(dr - asin^2\theta\varphi) + \rho^2(d\theta^2 - sin^2\theta\varphi^2)} \quad (5)$$

The Kerr metric or Kerr geometry describes the geometry of empty spacetime around a rotating uncharged axially-symmetric black hole with a spherical event horizon. The Kerr metric is a generalization of the Schwarzschild metric, and an exact solution of the Einstein field equations of general relativity [10]

Starting in the 1970s theoretical work led to the understanding of black hole quasi-normal modes, and in the 1990s higher-order post Newtonian calculations preceded extensive analytical studies of relativistic two-body dynamics. These advances, together with numerical relativity breakthroughs in the past decade, have enabled modeling of binary black hole mergers and accurate predictions of their gravitational waveforms.

2.1 Effect of GW

The characteristics of gravitational radiation can be seen from the perturbation of space-time. And in the weak field approximation, it is expressed by,

$$\boldsymbol{h_{\mu\nu} = g_{\mu\nu} - \eta_{\mu\nu}} \quad (6)$$

Where $h_{\mu\nu}$ is the perturbation from Minkowski Space. The detailed information about the gravitational wave is carried in the form of the quantity $h_{\mu\nu}$. There is freedom of the choice of gauge, but in the transverse traceless gauge and weak field limit, the field equations become a wave equation.

$$\boldsymbol{\left(\nabla^2 - \frac{1}{c^2}\frac{\partial^2}{\partial t^2}\right)h_{\mu\nu} = 0} \quad (7)$$

With the solution being plane waves having two polarizations for the gravitational wave,

$$\boldsymbol{h_{\mu\nu} = ah_+\left(t - \frac{z}{c}\right) + bh_\times\left(t - \frac{z}{c}\right)} \quad (8)$$

A gravitational wave propagating in the z-direction takes the form.

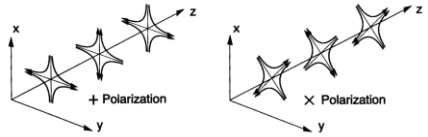

Fig. 2 Lines of force for plane gravitational waves propagating along the z axis

From fig.2 the wave on the left is purely in the +polarization state, and the one on the right is purely in the × polarization state. The gravitational waves produce tidal forces in planes transverse to the propagation direction [11].

With the condition that $\boldsymbol{h_{\mu\nu}}$is symmetric and traceless, the Einstein field equation reduces to just two components. The two degrees of freedom, $\boldsymbol{h_+}$ and $\boldsymbol{h_\times}$, are known as the plus (+) and cross (×) polarizations, respectively. A gravitational wave in this gauge could consist of either polarisation alone or a combination of the two [12].

Hence the effect of a passing gravitational wave on a ring of particles can be seen in Fig.1 by observing the change in proper distance between two test particles for both polarizations.

2.2 Direct Detection of GW

Experiments to detect gravitational waves began with Weber and his resonant mass detectors in the 1960s [13], followed by an international network of cryogenic resonant detectors (Astone et al., 2010). Interferometric detectors were first suggested in the early 1960s and the 1970s. A study of the noise and performance of such detectors [14] and further concepts to improve them, led to proposals for long-baseline broadband laser interferometers with the potential for significantly increased sensitivity ([15]. By the early 2000s, a set of initial detectors was completed, including TAMA 300 in Japan, GEO 600 in Germany, the Laser Interferometer Gravitational-Wave Observatory (LIGO) in the United States, and Virgo in Italy. Combinations of these detectors made joint observations from 2002 through 2011, setting upper limits on a variety of gravitational-wave sources while evolving into a global network. In 2015, Advanced LIGO became the first of a significantly more sensitive network of advanced detectors to begin observations [16]. In addition, the LISA project (LISA Pathfinder) for a space interferometer was launched on December 3, 2015 and dedicated to an end-to-end experimental demonstration of the free fall of test masses (TMs) at the level required for a future space-based gravitational wave (GW) observatory [17]. Advanced LIGO has on December 26, 2015, observed gravitational wave ripples in the fabric of spacetime for the second time. The gravitational waves were detected by both twin Laser Interferometer Gravitational-Wave Observatory (LIGO) detectors, located in Livingston, Louisiana, and Hanford, Washington, USA.

It is significant that these black holes were much less massive than those observed in the first detection, says Gabriela Gonzalez, LIGO Scientific Collaboration (LSC) spokesperson and professor of physics and astronomy at Louisiana State University. "Because of their lighter masses compared to the first detection, they spent more time-about one second-in the sensitive band of the detectors. It is a promising start to mapping the populations of black holes in our universe" [18].

During the merger, which occurred approximately 1.4 billion years ago, a quantity of energy roughly equivalent to the mass of the sun was converted into gravitational waves. The detected signal comes from the last 27 orbits of the black holes before their merger. Based on the arrival time of the signals with the Livingston detector measuring the waves 1.1 milliseconds before the Hanford detector; the position of the source in the sky can be roughly determined.

Soon, Virgo, the European interferometer, will join a growing network of gravitational wave detectors, which work together with ground-based telescopes that follow-up on the signals, notes Fulvio Ricci, the Virgo Collaboration spokesperson, a Physicist at Istituto Nazionale di Fisica Nucleare (INFN) and professor at Sapienza University of Rome. "The three interferometers together will permit a far better localization in the sky of the signals [18].

2.3 Sensitivity of Interferometers

Ground-based interferometric GW observatories measure the presence of a GW via extremely small phase differences of two interfering laser beams with a fractional change of the order of $h \sim 10^{-21}$. LIGO has defined an upgrade goal called Advanced LIGO. Advanced LIGO gravitational wave interferometers and their international partners have sensitivities $h+ \sim h\times \sim 10^{-22}$ of frequency $1\leq f \leq 10^4$ Hz. LISA has an armlength of $5x10^6$ Km capable of detecting GWs strain of amplitude $h = \Delta L/L \sim 10^{-24}$ in the low-frequency band, $10^{-6} \leq f \leq 1$Hz.

To be able to measure these small changes, the effective optical path needs to be increased. This is commonly done by adding additional input test masses to build a Fabry-Perot cavity. Secondly, all other noise sources which cause phase differences need to be well understood in order not to confuse their contributions with a real gravitational wave. The main noise sources for ground-based detectors are seismic noise, thermal noise, shot noise, radiation pressure noise and gravity gradient noise. There are many more noise sources and some of them are poorly understood. The sum of all noise contributions defines the sensitivity of the detector, which is characterized by the noise power spectral density (PSD). Despite its dimension being time, more commonly the units Hz^{-1} are used. The square root of the PSD is referred to as the noise amplitude with dimension $Hz^{-1/2}$ [19].

3.0 Framework

General relativity is a theory of gravity that is consistent with special relativity in many respects, and with the principle that nothing travels faster than light. This means that changes in the gravitational field cannot be felt everywhere instantaneously: they must propagate. In general relativity they propagate at the same speed as vacuum electromagnetic waves: the speed of light. These propagating changes are called gravitational waves. However, general relativity is a non-linear theory and there is, in general, no sharp distinction between the part of the metric that represents the waves and rest of the metric. Only in certain approximations can we clearly define gravitational radiation. Three interesting approximations in which it is possible to make this distinction are:

- linearized theory.
- Small perturbations of a smooth, time-independent background metric.
- Post-Newtonian (PN) theory.

The simplest starting point for our discussion is certainly linearized theory, which is a weak-field approximation to general relativity, where the equations are written and solved in a nearly flat space-time. The static and wave parts of the field cleanly separate. We idealize gravitational waves as a "ripple" propagating through a flat and empty universe.

This picture is a simple case of the more general "short-wave approximation", in which waves appear as small perturbations of a smooth background that is time-dependent and whose radius of curvature is much larger than the wavelength of the waves. This approximation describes wave propagation well, but it is inadequate for wave generation.

The most useful approximation for sources is the post-Newtonian approximation, where waves arise at a high order in corrections that carry general relativity away from its Newtonian limit. For nearly Newtonian sources the post-Newtonian approximation provides a good framework for calculating gravitational waves.

\3.1 Description of Mathematical Model

The fundamental geometrical framework of relativistic metric theories of gravity is spacetime, which mathematically can be described as a four-dimensional manifold whose points are called events. Every event is labeled by four coordinates $\boldsymbol{x^{\mu}}(\mu = 0,1,2,3)$; the three coordinates $\boldsymbol{x^{i}}(\boldsymbol{i} = 1,2,3)$ give the spatial position of the event, while $\boldsymbol{x^{0}}$ is related to the coordinate time $\boldsymbol{t}(\boldsymbol{x^{0}} = \boldsymbol{ct}$, where c is the speed of light,).

The choice of the coordinate system is quite arbitrary and coordinates transformations of the form $\boldsymbol{\tilde{x}^{\mu}} = \boldsymbol{f^{\mu}}(\boldsymbol{x^{\lambda}})$ are allowed. The motion of a test particle is described by a curve in spacetime. The distance $\boldsymbol{ds}$ between two neighboring events, one with coordinates $\boldsymbol{x^{\mu}}$ and the other with coordinates $\boldsymbol{x^{\mu}} + \boldsymbol{dx^{\mu}}$, can be expressed as a function of the coordinates via a symmetric tensor $\boldsymbol{g_{\mu\nu}}(\boldsymbol{x^{\lambda}}) = \boldsymbol{g_{\nu\mu}}(\boldsymbol{x^{\lambda}})$, i.e.,

$$\boldsymbol{ds^2} = \boldsymbol{g_{\mu\nu}} \boldsymbol{dx^{\mu}} \boldsymbol{dx^{\nu}} \tag{9}$$

This is a generalization of the standard measure of distance between two points in Euclidian space. For the Minkowski spacetime (the spacetime of special relativity),

$$g_{\mu\nu} \equiv \eta_{\mu\nu} = \begin{pmatrix} -1 & 0 & 0 & 0 \\ 0 & 1 & 0 & 0 \\ 0 & 0 & 1 & 0 \\ 0 & 0 & 0 & 1 \end{pmatrix} \quad (10)$$

The symmetric tensor is called the metric tensor or simply the metric of the spacetime. In general relativity, the gravitational field is described by the metric tensor alone, but in many other theories one or more supplementary fields may be needed as well. In what follows, we will consider only the general relativistic description of gravitational fields, since most of the alternative theories fail to pass the experimental tests.

The information about the degree of curvature (i.e., the deviation from flatness) of a spacetime is encoded in the metric of the spacetime. According to general relativity, any distribution of mass bends the spacetime fabric and the Riemann tensor $R_{\mu\nu}$ (that is a function of the metric **tensor** $g_{\mu\nu}$ and of its first and second derivatives) is a measure of the spacetime curvature.

In this research, we will consider mass distributions, which we will describe by the stress-energy tensor $T_{\mu\nu}(x^{\lambda})$.

Einstein's gravitational field equations connect the curvature (Einstein) tensor and the stress-energy tensor $T_{\mu\nu}$ through the fundamental relation,

$$G_{\mu\nu} = R_{\mu\nu} - \frac{1}{2} g_{\mu\nu} R = kT_{\mu\nu} \quad (11)$$

This means that the gravitational field, which is directly connected to the geometry of spacetime, is related to the distribution of matter and radiation in the universe. $R_{\mu\nu}$ is the so- called Ricci tensor and comes from a contraction of the Riemann tensor, R is the scalar curvature, while $G_{\mu\nu}$ is the so-called Einstein tensor, $k = 8\pi G/c^4$ is the coupling constant of the theory and **G** is the gravitational constant. The vanishing of the Ricci tensor corresponds to a spacetime free of any matter distribution. However, this does not imply that the Riemann tensor is zero. Therefore, in the empty space far from any matter distribution, the Ricci tensor will vanish while the Riemann tensor can be nonzero; this means that the effects of a propagating gravitational wave in an empty spacetime will be described via the Riemann tensor.

3.2 Gravitational Waves in Linearized Gravity

The most straightforward way to obtain gravitational waves is to work in the theory of linearized gravity. Within this framework, it is assumed that spacetime, described by the metric tensor, is approximately flat. In other words, it is decomposed into the flat Minkowski metric $\eta_{\mu\nu}$ and some contribution $h_{\mu\nu}$.

$$g_{\mu\nu} = \eta_{\mu\nu} + h_{\mu\nu} \quad (12)$$

Since the spacetime is approximately flat, this contribution must be small. As a result, in calculating physically significant quantities only terms up to linear order in $h_{\mu\nu}$will be kept

$$||h_{\mu\nu}|| << 1 \quad (13)$$

Equation 3.3 is not a simple expression to work with; it would be suitable to reduce the Einstein equation to something more useful. One way of doing this is to cease working with $h_{\mu\nu}$ and instead work with an expression that is known as the trace-reversed metric. It is defined as

$$\bar{h}_{\mu\nu} = h_{\mu\nu} - \frac{1}{2} g_{\mu\nu} h \quad (14)$$

and its name stems from the fact that its trace is the opposite of the original metric.

Choosing the trace-reverse of $h_{\mu\nu}$ and the Lorentz condition,

$$\delta^{\mu} \bar{h}_{\mu\nu} = 0 \quad (15)$$

We find the linearized Einstein Field Equation can be written elegantly as

$$\Box \bar{h}_{\mu\nu} = -2kT_{\mu\nu} \quad (16)$$

where

$= \delta^{\mu}\delta_{\mu}$ is the flat space d'Alambertian.

$k = 8\pi G/c^4$

Therefore,

$$\Box \bar{h}_{\mu\nu} = \left(-\frac{1}{c^2}\frac{\partial^2}{\partial t^2} + \nabla^2\right)\bar{h}_{\mu\nu} = -\frac{16\pi G T_{\mu\nu}}{c^4} \quad (17)$$

In order to study the propagation of gravitational waves and their interaction with test masses, we are interested in the governing equations outside the source, i.e.$T_{\mu\nu} = 0$:

$$\Box \bar{h}_{\mu\nu} = 0 \quad (18)$$

In the vacuum case, the Lorenz gauge condition alone is not enough to fix the gauge freedom. Further inspection shows that the Lorenz gauge condition is not violated by imposing $\bar{h} = 0$, then $\bar{h}_{\mu\nu} \equiv h_{\mu\nu}$, and $h^{0i} = 0$. The Lorenz condition then becomes

$$\partial^0 h_{00} = 0 \quad (19)$$

$$\partial^i h_{ij} = 0 \quad (20)$$

This means that h_{00} corresponds to the static (time-independent) part of the gravitational field; the time-varying gravitational degrees of freedom, the GW itself, is contained in the time-dependent components h^{0i}.

By via exploiting the gauge degrees of freedom we have set

$$h^{0\mu} = 0 \quad (21)$$

$$h^i{}_i = 0 \quad (22)$$

$$\partial^0 h_{ij} = 0 \quad (23)$$

This set of conditions defines the transverse-traceless gauge (TT gauge), the most convenient gauge to express gravitational waves outside the source. The general complex solutions of equation (17) are plane-wave solutions

$$h_{\mu v} = A_{\mu v} e^{ik_\sigma x^\sigma} \quad (24)$$

with $k^\mu = \omega, k^i$ the wave vector. In the TT-gauge this general expression can be rewritten as

$$h_{ij}{}^{TT} = e_{ij} e^{ik_\mu x^\mu} \quad (25)$$

Where e_{ij} is the polarization tensor, and k_μ is the wave vector.

3.3 Estimated Frequency of Emitted Gravitational Wave

Consider two stars of mass m_1 and m_2 such that, $M=m_1+m_2$ in a circular orbit in the x-y plane, at distance $R=a_1+a_2$ from their common center of mass (Fig 3).

Treating the motion of the stars in the Newtonian approximation; circular orbits are most easily characterized by equating the force due to gravity to the outward "centrifugal" force:

$$\frac{GM^2}{R^2} = \frac{Mv^2}{R} \quad (26)$$

This gives,

$$v = \left(\frac{GM}{R}\right)^{1/2} \quad (27)$$

The time it takes to complete a single orbit is simply,

$$T = \frac{2\pi R}{v} \quad (28)$$

But more useful is the angular frequency of the orbit.

$$\Omega = \frac{2\pi}{\mathrm{T}} = \left(\frac{GM}{R^3}\right)^{1/2} \quad (29)$$

The most numerous sources of gravitational waves are binary stars systems. In just half an orbital period, the non-spherical part of the mass distribution returns to its original configuration, so the angular frequency of the emitted gravitational waves is twice the orbital angular frequency [20].

Therefore, we have,

$$f_{gw} = 2\Omega \quad (30)$$

Using (30), the estimated frequency of **PSR B1913+16** with its parameters as;

$T = 465 \times 60 = 27900$s

but,

$$\Omega = \frac{1}{T}$$

$$\Rightarrow \Omega = \frac{1}{27900} = 3.584 \times 10^{-5} \text{ Hz}$$

Therefore,

$$f_{gw} = 2\Omega = 2 \times 3.584 \times 10^{-5} = 7.178 \times 10^{-5} \text{ Hz}$$

Meanwhile, the estimated frequencies of (XTE J1118+480, 1915+105, Nova Scopii, V4641 Sgr, and VFTS 352) were equally obtained from the same relation (30) and presented in table 1.

3.4 Luminosity in Gravitational Waves

According to Sathyaprakash and Schutz (2009), the energy carried by the gravitational wave must be proportional to the square of the time-derivative of the wave amplitude, so it will depend on the sum of the squares of the components $\ddot{I}_{ij}$. The energy flux falls off as $\frac{1}{r^2}$, but when integrated over a sphere of radius r to get the total luminosity, the dependence on r goes away, as it should. The luminosity contains a factor G/c^5 on dimensional grounds, and a further factor of 1/5 comes from a careful calculation in general relativity. The result is the gravitational wave luminosity in the quadrupole approximation:

$$\boldsymbol{L_{gw} = -\frac{dE}{dt} = \frac{1}{5}\frac{G}{C^5}\langle \dddot{I}_{ij}\dddot{I}_{ij}\rangle} \quad (31)$$

where the angle brackets denote averages over regions of the size of a wavelength and times of the length of a period of the wave.

If we assume that the two bodies making up the binary lie in the $\boldsymbol{x-y}$ plane and their orbits are circular (see Figure 2),

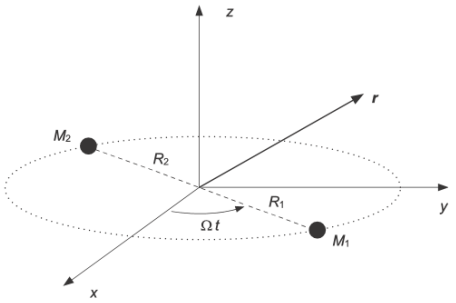

Fig. 3 Coordinate system for binary stars in circular orbits

then introducing polar coordinates for the center of mass for the first mass,

$$\boldsymbol{x(t) = Rcos\Omega t, y(t) = sin\Omega t} \text{ and } \boldsymbol{z(t) = 0} \quad (32)$$

the components of the second mass moment are given by,

$$\boldsymbol{I_{ij} = \int \rho(t, x')x_i x_j d^3 x_\mu} \quad (33)$$

which reduces to,

$$\boldsymbol{I_{ij} = \psi R^2 x_i(t) x_j(t)} \quad (34)$$

for two discrete masses.

Explicitly, the non-zero components are,

$$\boldsymbol{I_{xx} = \psi R^2 cos^2\Omega t,\ I_{yy} = \psi R^2 sin^2\Omega t,\ I_{xy} = I_{yx} = \psi R^2 \sin\Omega t \cos\Omega t} \quad (35)$$

Noting that

$$\boldsymbol{cos^2\Omega t = \frac{1}{2}(1 + cos2\Omega t), sin^2\Omega t = \frac{1}{2}(1 - cos2\Omega t), and\ \sin\Omega t\cos\Omega t = \frac{1}{2}sin2\Omega t} \quad (36)$$

And evaluating the double time derivative, we obtain

$$\boldsymbol{\ddot{I}_{xx} = -2\Omega^2\psi R^2 cos2\Omega t, \ddot{I}_{yy} = 2\Omega^2\psi R^2 cos2\Omega t, \ddot{I}_{xy} = \ddot{I}_{yx} = -2\Omega^2\psi R^2 sin2\Omega t} \quad (37)$$

and the corresponding expressions for the other components, the triple time derivatives are

$$\boldsymbol{\dddot{I}_{xx} = 4\Omega^3\psi R^2 sin2\Omega t, \dddot{I}_{yy} = -4\Omega^3\psi R^2 sin2\Omega t, \dddot{I}_{xy} = \dddot{I}_{yx} = -4\Omega^3\psi R^2 cos2\Omega t} \quad (38)$$

Thus, we have

$$\boldsymbol{L_{gw} = \frac{1}{5}\frac{G}{C^5}\langle \dddot{I}_{ij}\dddot{I}_{ij}\rangle = \frac{1}{5}\frac{G}{C^5}\langle (\ddot{I}_{xx})^2 + 2(\ddot{I}_{xy})^2 + (\ddot{I}_{yy})^2\rangle}$$

$$\boldsymbol{= \frac{1}{5}\frac{G}{C^5}\left[\int_0^P \left((\ddot{I}_{xx})^2 + 2(\ddot{I}_{xy})^2 + (\ddot{I}_{yy})^2\right) dt\right]}$$

$$\boldsymbol{= \frac{16}{5P}\Omega^6\psi^2 R^4 \int (sin^2 2\Omega t + 2cos^2 2\Omega t + sin^2 2\Omega t) dt}$$

$$\boldsymbol{= \frac{32}{5}\frac{G}{C^5}\Omega^6\psi^2 R^4 = \frac{32}{5}\frac{G^4}{C^5}\frac{M^3\psi^2}{R^5} = \frac{32}{5}\frac{G^4}{C^5}\frac{(m_1 m_2)^2(m_1+m_2)}{R^5}} \quad (39)$$

From the expression of (39) the estimated luminosity for **PSR B1913+16** with its parameters is thus obtained as:

$$\boldsymbol{L_{gw} = \frac{32}{5}\frac{G^4}{C^5}\frac{(m_1 m_2)^2(m_1+m_2)}{R^5}}$$

$$\frac{G^4}{C^5} = 8.188 \times 10^{-84}$$

$$(m_1 m_2)^2 = (7.84 \times 10^{60})(7.84 \times 10^{60})$$

$$(m_1 + m_2) = 5.6 \times 10^{30} \text{ kg}$$

At the time of coalesce,

$$R_s = \frac{2GM}{C^2}$$

Where R_s is the separation between the two masses.

$$\Rightarrow R_s = \frac{2(6.673 \times 10^{-11})(5.6 \times 10^{30})}{(3 \times 10^8)^2} = 8304.111\text{m}$$

Therefore,

$$\boldsymbol{L_{gw}} = \frac{32}{5}\frac{(8.188\times10^{-84})(7.84\times10^{60})^2(5.6\times10^{30})}{(8304.111)^5}$$

$$\boldsymbol{L_{gw}} = 2.284\times10^{51}\text{erg/s}$$

The luminosity for XTE J1118+480, 1915+105, Nova Scopii, V4641 Sgr, and VFTS 352 were obtained using same expression (39) and presented in table (2)

3.5 Expected Time of Merger of Binary Black Holes

Another "centrifuge" is a binary star system. The radiation of energy by the orbital motion causes the orbit to shrink. The shrinking will make any observed gravitational waves increase in frequency with time [1].

If we assume that the two bodies $\boldsymbol{m_1}$ and $\boldsymbol{m_2}$ making up the binary lie in the $x-y$ plane at distances $\boldsymbol{a_1}$ and $\boldsymbol{a_2}$ from the center of mass (as shown in Fig 3), their orbits are circular and rotating at angular frequency Ω.

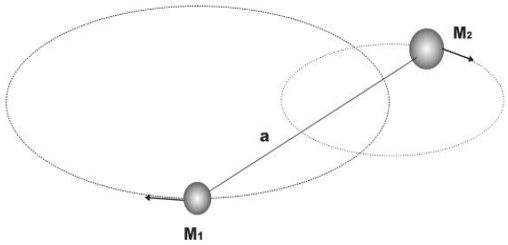

Fig. 4 Binary Star System

where $\boldsymbol{a} = \boldsymbol{a}_1 + \boldsymbol{a_2}$, $\boldsymbol{a_1 m_1 = a_2 m_2 = a\psi}$. Here $\boldsymbol{\psi = m_1 m_2/M}$ is the reduced mass of the system and $\boldsymbol{M = m_1 + m_2}$ its total mass.

The total energy of the binary system can be written as

$$\boldsymbol{E} = \left(\frac{1}{2}\boldsymbol{m_1 a_1}^2 + \frac{1}{2}\boldsymbol{m_2 a_2}^2\right)\boldsymbol{\Omega^2} - \frac{\boldsymbol{Gm_1 m_2}}{\boldsymbol{a}} = -\frac{1}{2}\frac{\boldsymbol{G\psi M}}{\boldsymbol{a}} \quad (40)$$

As the gravitating system loses energy by emitting radiation, the distance between the two bodies shrinks at a rate,

$$\frac{\boldsymbol{dE}}{\boldsymbol{dt}} = \frac{1}{2}\frac{\boldsymbol{G\psi M}}{\boldsymbol{a^2}}\frac{\boldsymbol{da}}{\boldsymbol{dt}} \quad (41)$$

Using equation 39

$$\frac{1}{2}\frac{\boldsymbol{G\psi M}}{\boldsymbol{a^2}}\frac{\boldsymbol{da}}{\boldsymbol{dt}} = \frac{32}{5}\frac{\boldsymbol{G^4}}{\boldsymbol{C^5}}\frac{\boldsymbol{M^3\psi^2}}{\boldsymbol{R^5}} \quad (42)$$

Since $\boldsymbol{a = R}$,

$$\frac{\boldsymbol{da}}{\boldsymbol{dt}} - \frac{64}{5}\frac{\boldsymbol{G^3}}{\boldsymbol{C^5}}\frac{\boldsymbol{M^2\psi}}{\boldsymbol{a^3}} \quad (43)$$

and the orbital frequency increases accordingly.

If, the present separation of the two stars is $\boldsymbol{a_0}$, then the binary system will coalesce after a time,

$$\int_{t_0}^{t}\boldsymbol{dt} = \int\frac{5}{64}\frac{\boldsymbol{c^5}}{\boldsymbol{G^3}}\frac{\boldsymbol{a^3}}{\boldsymbol{M^2\psi}}\boldsymbol{da} \quad (44)$$

Finally,

$$\boldsymbol{t} = \frac{5}{256}\frac{\boldsymbol{c^5}}{\boldsymbol{G^3}}\frac{\boldsymbol{a^4}}{\boldsymbol{M^2\psi}} = \frac{5}{256}\frac{c^5}{G^3}\frac{R^4}{(m_1m_2)(m_1+m_2)} \quad (45)$$

Therefore, using (45) the estimated time of merger for **PSR B1913+16** with its parameters is obtained as:

$$\frac{c^5}{G^3} = 8.178\times10^{72}$$

$$(m_1m_2) = (1.781\times10^{62})\text{kg}^2$$

$$(m_1+m_2) = 2.67\times10^{31}\text{ kg}$$

$$R = 1.95\times10^{9}\text{m}$$

Substituting these values into the equation yields:

$$t = \frac{5}{256}\frac{(8.178\times10^{72})(1.95\times10^{9})^4}{(1.781\times10^{62})(2.67\times10^{31})}$$

$$t = 4.864\times10^{14}\text{s}.$$

Similarly, for XTE J1118+480, 1915+105, Nova Scopii, V4641 Sgr, and VFTS 352 were obtained using same expression (45) and presented in table (3)

4.0 Results

The estimated values of frequency, luminosity, and time of merger of binary black holes obtained from different galaxies with qualitative behavior of compact binary coalescences within the post-Newtonian framework. The following are the selected binary systems: PSR 1913+16, XTE J1118+480, 1915+105, Nova Scopii, V4641 Sgr, and VFTS 352 and their companions. The parameters considered includes the distance r (observer distance), R (orbital separation), masses M ($M_{\odot}$). The results obtained from the estimation of binary black hole parameters are presented in the tables 1, 2, and 3.

Table 1: Estimated parameters of Frequency of GW

Source	T(s)	Ω(Hz)	f_{gw} (Hz)
PSR 1913+16	27900	3.584×10^{-5}	7.178×10^{-5}
PSR 1913+16	27900	3.584×10^{-5}	
XTE J1118+480	354240	2.823×10^{-6}	5.646×10^{-6}
XTE J1118+480	354240	2.823×10^{-6}	
GRS 1915+105	2894400	3.455×10^{-7}	6.91×10^{-7}
GRS 1915+105	2894400	3.455×10^{-7}	
Nova Scopii	226714	4.411×10^{-6}	8.8222×10^{-6}
Nova Scopii	226714	4.411×10^{-6}	
V4641 Sgr	243389	4.109×10^{-6}	8.217×10^{-6}
V4641 Sgr	243389	4.109×10^{-6}	
VFTS 352	97114	1.030×10^{-5}	2.06×10^{-5}
VFTS 352	97114	1.030×10^{-5}	

Table 2: Estimated parameters of luminosity at the time of merger

Source	Mass ($\times 10^{30}$) Kg	R_s (m)	L_{gw} ($\times 10^{50}$) erg/s
PSR 1913+16	2.8	4150	145.8
PSR 1913+16	2.8	4150	
XTE J1118+480	12.2	39593	4.539
XTE J1118+480	13.7	39593	
GRS 1915+105	19	99354	0.717
GRS 1915+105	28	99354	
Nova Scopii	10.8	20316	2.025
Nova Scopii	2.9	20316	
V4641 Sgr	19.22	47868	4.220
V4641 Sgr	13.06	47868	
VFTS 352	57.26	170532	4.539
VFTS 352	57.70	170532	

Table 3: Estimated parameters time of merger

Source	Mass ($\times 10^{30}$) Kg	R ($\times 10^{10}$) m	t (s)
PSR 1913+16	2.8	0.665	7.13×10^{18}
PSR 1913+16	2.8	0.665	
XTE J1118+480	12.2	0.195	4.864×10^{14}
XTE J1118+480	13.7	0.195	
GRS 1915+105	19	6.612	6.114×10^{20}
GRS 1915+105	28	6.612	
Nova Scopii	10.8	1.058	4.671×10^{18}
Nova Scopii	2.9	1.058	
V4641 Sgr	19.22	1.485	9.601×10^{17}
V4641 Sgr	13.06	1.485	
VFTS 352	57.26	0.194	6.013×10^{12}
VFTS 352	57.70	0.194	

5.0 Discussion

The estimated values of GW frequency obtained in table 1 indicated a high sensitivity that could be suitable within the detector's frequency band, such as LISA. The values indicate that these BBH are suitable candidates for GW detectors. The estimated values of frequencies of $10^{-5} - 10^{-7}$Hz shows an excellent sensitivity for LISA.

The LIGO's system reached a peak gravitational-wave luminosity of 3.6×10^{56}erg/s equivalent to $200M_{\odot}C^2$. Meanwhile the estimated values obtained as indicated in figure 2 is between 145.8×10^{50} - 0.717×10^{50} erg/s which gives a significant gravitational- wave luminosity of the sources BBH. Meanwhile, the estimated time of merger for the source stars indicated in figure 3 reveals to be between10^{12} - 10^{20}s.

The LIGO observatories has a range of detectable signals of GW amplitude as h ~ 1.0 $x10^{-21}$ and h ~ 3.3 $x10^{-22}$ when GW150914 and GW151226 were detected. These observations were made at signal frequencies of f ~ 35 – 350 Hz and 35 – 450 Hz by the aLIGO. However, the estimated values displayed in fig (1) indicates that the BBH such as XTE J1118+480, mass of 13 x 10^{30} kg -13.7 kg with h ~ 3.410 x 10^{-21}; Nova Scopii mass between 10.8 x 10^{30} kg – 2.9 x 10^{30} Kg and h ~ 2.29 x 10^{-23}; V4641 Sgr mass of 13.06 x 10^{30} kg - 19.22 x 10^{30} Kg and h ~ 1.174 $x10^{-22}$; VFTS 352 mass 57.26 x 10^{30} Kg, h ~ 1.45 x 10^{-22} are suitable sources for GW detection by aLIGO detectors as their amplitudes lies within the sensitive signal band.

However, the technology built for all ground base interferometric detectors operates within the frequency band of $10^1 – 10^4$ Hz. Hence, in comparison with the estimated values from table 1 shows $10^{-5} – 10^{-7}$ Hz which is best for detection by LISA.

6.0 Conclusion

Gravitational waves are perhaps the most elusive prediction of Einstein's theory, one that he and his contemporaries debated for decades. According to his theory, space and time form a stretchy fabric that bends under heavy objects, and to feel gravity is to fall along the fabric's curves. Einstein flip-flopped, confused as to what his equations implied. But even steadfast believers assumed that, in any case, gravitational waves would be too weak to observe.

The detection ushers in a new era of gravitational-wave astronomy that is expected to deliver a better understanding of the formation, population, and galactic role of black holes which the results obtained in the estimation of the parameters has shown (see table1,2 & 3).

We conclude that these results are potentially measurably by the LISA operating at its projected design sensitivity.

7.0 References

[1] Schutz, B. F. (2000). Gravitational Radiation. Max Planck Institute for Gravitational Physics The Albert Einstein Institute Potsdam, Germany: arXiv:gr-qc/0003069v1 [gr-qc]

[2] Patricia, S, (2014). Studying and Modelling the Complete Gravitational – Wave Signal from Processing Black Hole Binaries. Retrieved from www.cardiff.edu/research on 17 th June, 2016.

[3] Belczynski K., Vassiliki K. and Tomasz B. (2002) Comprehensive Study of Binary Compact Objects as Gravitational Wave Sources: Evolutionary Channels, Rates, and Physical Properties. The Astrophysical Journal, 572:407–431.

[4] Taylor, J. H.; Weisberg, J. M. (1989). Further experimental tests of relativistic gravity using the binary pulsar PSR 1913 + 16. Astrophysical Journal, Part 1 (ISSN 0004-637X), vol. 345

[5] Hulse, R. and Taylor, J. (1975). *Discovery of a Pulsar in a Binary system*. Astrophysical Journal, 195; DOI. 10.1086/181708.

[6] Miller, J. M., Fabian, A. C., and Miller M. C. (2004). A comparison of intermediate mass black hole candidate ULXS and stellar-mass black holes. Retrieved from www.arXiv:astro-ph/0406656v2 on 17/06/2016

[7] Scott B. (2015). Gravitational wave searches associated with Galactic core-collapse supernovae Coughlin Submitted for the degree of Masters of Philosophy School of Physics and Astronomy Cardiff University,July 2015)Retrieved from www.cardiff.edu/research

[8] Abbott**,** B. P. *et al.* (LIGO Scientific Collaboration and Virgo Collaboration) (2016b)**.** GW151226: Observation of Gravitational Waves from a 22-Solar-Mass Binary Black Hole Coalescence.Phys. Rev. Lett. 116, 241103 – Published 15 June 2016.

[9] Marko V. (2010) .Schwarzschild Solution In General Relativity NASA (2016): http://www.nasa.gov/audience/forstudents/k-4/stories/nasa-knows/what-is-a-black-hole-k4.html on 13/06/2016, @ 1:52am

[10] Christian H. and Friedrich W. H. (2015). Schwarzschild and Kerr Solutions of Einstein's Field Equation. arXiv:1503.02172v1 [gr-qc] Phys. Rev. D.88.043007.

[11] Armano, M. et al. (2016) Sub-Femto-g Free Fall for Space-Based Gravitational Wave Observatories. LISA Pathfinder Results. Physical Review Letters. PRL 116, 231101.

[12] Accadia, F. Acernese, M. Alshourbagy. (2012). Virgo: a laser interferometer to detect gravitational waves. http://iopscience.iop.org/1748-0221/7/03/P03012

[13] Weber, J. (1960) Detection and Generation of Gravitational Waves. Phys. Rev(10.1103/PhysRev.117.306)

[14] Astone, P. *et al.*IGEC2: A 17-month search for gravitational wave bursts in 2005–2007 Phys. Rev. D **82**, 022003. American Physical Society doi 10.1103/PhysRevD.82.022003

[15] Weiss, R. (1972,) Electromagnetically coupled broadband gravitational antenna, Quarterly Report of the Research Laboratory for Electronics, MIT Report No. 105, https:// dcc.ligo.org/LIGO-P720002/public/main

[16] Drever, R. W. P., Raab, F. J., Thorne, K. S. Vogt, R. and Weiss, R. (1989). Laser Interferometer Gravitational-wave Observatory (LIGO) Technical Report, https://dcc.ligo.org/ LIGO-M890001/public/main

[17] Aso, Y., Michimura, Y., Somiya, K., Ando, M., Miyakawa, O., Sekiguchi, T., Tatsumi, D. and Yamamoto, H. (2013). Interferometer design of the KAGRA gravitational wave detector.

[18] LIGOCaltech.(2016)https://www.ligo.caltech.edu/system/media_files/binaries/303/original/ligo-educators-guide

[19] Shoemaker, David and Losurdo, Giovanni. Possible scenarios for commissioning and early observing with the second generation detectors. Technical Report LIGO-G10001760-v7, LIGO Project, 2010. URL https://dcc.ligo.org/DocDB/0009/G1000176/007/Advanced%20Virgo%

[20] Schutz B.F. & Ricci, F. (2010). Gravitational Waves, Sources and Detectors. Department of Physics and Astronomy Cardiff University, Wales: arXiv:1005.4735v1 [gr-qc]